

UKAEA

Preprint

# THE LASER HARDENING OF RING GROOVES IN MEDIUM-SPEED DIESEL ENGINE PISTONS

A. S. BRANSDEN  
S. T. GAZZARD  
B. C. INWOOD  
J. H. P. C. MEGAW

CULHAM LABORATORY  
Abingdon Oxfordshire

1985



This document is intended for publication in a journal or at a conference and is made available on the understanding that extracts or references will not be published prior to publication of the original, without the consent of the authors.

Enquiries about copyright and reproduction should be addressed to the Librarian, UKAEA, Culham Laboratory, Abingdon, Oxon. OX14 3DB, England.

## THE LASER HARDENING OF RING GROOVES IN MEDIUM-SPEED DIESEL ENGINE PISTONS

A.S. Bransden\*, S.T. Gazzard\*\*, B.C. Inwood\*\* and J.H.P.C. Megaw\*

### ABSTRACT

Internal combustion engine durability is enhanced if the side faces of the ring-grooves in the pistons have a wear-resistant surface. The present work concerns the development of a technique to achieve local hardening of medium-speed steel-crowned and cast iron pistons, based on use of a 5kW industrial laser. Specific aspects of the development which are discussed include: beam coupling and choice of absorbing coatings, choice of beam power density/interaction time, metallurgy, treatment of the edges of external corners, back-tempering, and induced distortion and surface changes. The work has resulted in the treatment of prototype pistons for evaluation in engine trials.

Paper submitted to the 4th International Congress on Heat Treatment of Materials, West Berlin, June 3-7, 1985. Congress organised by the Arbeitsgemeinschaft Wärmebehandlung und Werkstofftechnik.

---

\*UKAEA Culham Laboratory, Abingdon, Oxon, OX14 3DB, UK

\*\* Wellworthy Ltd, Lympington, Hants, SO4 9YE, UK



## 1. INTRODUCTION

Medium-speed diesel engines for industrial, marine and rail-traction applications with a bore-size typically in the range 170-400mm, have traditionally employed cast aluminium alloy pistons with integral reinforcement of the upper ring grooves. However, such engines have been rapidly uprated in recent years and this has led to the introduction of ferrous-crowned pistons into many new and existing engine designs, in order to improve durability under the increased thermal and mechanical loadings experienced.

The preferred piston for high duty applications is now of two-piece construction, with the body of forged aluminium alloy and the crown of forged chromium-molybdenum alloy steel, usually inclusion modified and in a martensitic condition. Alternatively, a lower-cost monolithic piston is employed, usually cast in a pearlitic nodular, or spheroidal graphite, iron. In both steel and iron, the combined ring and ring-groove side-face wear tends to limit the operational life and, particularly where lower-grade and wider cut fuels are used, this can fall far short of the 30-50,000 hours life required for cost-effective operation, unless additional wear protection is afforded.

Since the principal mechanism of wear is abrasive, localised transformation hardening of the groove surfaces by, for instance, induction hardening can provide the necessary protection. However, the use of induction hardening in this groove geometry favours the production of hardened zones which are deeper than that necessary for wear control, with the following consequences:-

- i. Due to the relatively high volume of material transformed, high internal stress may be generated in a region of the component subjected to high operational stresses.
- ii. Ring grooves must be reground after hardening in order to satisfy stringent surface finish and dimensional requirements.

In addition, pistons below about 250mm diameter are particularly difficult to treat due to the complexity of the inductors required. The objective of this programme was to develop alternative processing technology to effect the localised transformation hardening by means of laser heating. The cost-effective treatment of an extended range of cast iron and steel components was sought, hopefully with the components in the finish-machined condition.



## 2. LASER TRANSFORMATION HARDENING

The versatility of high power lasers is now well recognised and, using appropriate beam manipulation, a single device can be used for cutting, welding, hard-facing and localised transformation hardening. Laser cutting is now extensively employed in industry, and in addition high-volume production-line applications are found in: laser welding of gear clusters<sup>(1)</sup> and transmission components<sup>(2)</sup>; laser hard-facing of gas turbine components<sup>(3)</sup>; and laser transformation hardening of power-steering components<sup>(4)</sup> and diesel engine bores<sup>(5)</sup>. The most significant attributes of laser processing are the localisation, precision and controllability with which energy is delivered to the workpiece. Thus, although the conversion efficiency of electrical power to laser beam power is typically less than 10%, the overall process efficiency can be high because workpiece heating is minimised; as a corollary, distortion is very much reduced and the need for final machining may be eliminated.

In laser transformation hardening the beam energy is deposited in a thin absorbing coating pre-applied to the component. The highest temperature is experienced at the surface, and workpiece heating takes place by conduction inwards from the surface. A thin skin is austenitised and, when exposure to the beam ceases, quenching into the bulk of the component is normally sufficient to ensure transformation. Figure 1 shows the target case profile chosen for this work, together with the range of groove dimensions tackled. The technical aims of the programme were:

- i. To investigate and optimise using simple coupons effects associated with beam coupling and choice of absorbing coatings, choice of beam power density/interaction time, metallurgy, and treatment of the edge at an external corner.
- ii. To evaluate effects associated with back-tempering and induced distortion and surface changes using simulated components.
- iii. To treat production components for engine trials.

These aspects are dealt with in turn below, after a description of the equipment used.

### 3. THE EQUIPMENT

The laser treatment was carried out in the Laser Applications Group at UKAEA Culham Laboratory and utilised the 5kW carbon dioxide laser CL5, developed at Culham and now manufactured and sold under license by Ferranti plc of Dundee, Scotland. The unit is an industrially-rated fast transverse flow type having unstable cavity, gas flow and discharge current on orthogonal axes. The annular output beam of diameter 42mm is taken via a zinc selenide window to a workstation (part of a four workstation complex) approximately five metres away, where beam and workpiece manipulation are performed as shown in Figure 2.

The incoming beam is focused and projected to the workpiece via two oscillating mirrors having crossed axes of rotation. The size of heating pattern may be altered by variation of the vibrational amplitude of the mirrors, and an absorbing mask (also of variable size) is provided close to the work to define the usable beam. The workpieces (test coupons or full size pistons) were fixed to a variable speed turntable which in turn was positioned on a three axis co-ordinate table used for accurate workpiece alignment. Air jets and local fume extraction were provided for quenching (where necessary) and removal of coating debris respectively.

### 4. PROCESS DEVELOPMENT

#### 4.1 Coupling/Coatings

At temperatures below their melting points, clean metallic surfaces can reflect as much as 95-98% of incident infrared energy. This loss of coupling may be reduced by consideration of the state of polarisation of the laser beam<sup>(6)</sup>, its angle of incidence and by use of an absorbing coating.

Many high power CO<sub>2</sub> lasers, including CL5, generate a beam which is plane-polarised i.e. the electric field (E-vector) lies in a fixed plane defined as the plane of polarisation. Consider now such a beam directed at a surface at an arbitrary angle of incidence (defined as the angle between the beam and the normal to the surface): if the plane of polarisation (E-vector) lies parallel to the plane of incidence/reflection, it is referred to as a p-wave, while if the E-vector is perpendicular to that plane it is referred to as an s-wave. In general p-waves experience lower reflectivity than s-waves over the range of angles of incidence, and the reflectivity exhibits a minimum at

the Brewster angle. The effect is observed also in the special case of reflection from an absorbing coating, and thus to maximise coupling it is necessary to operate using p-wave configuration, aligned if possible at the Brewster angle.

In this work, groove geometry dictated the use of a beam with  $60^\circ$  angle of incidence. Tests on flat coupons coated with colloidal graphite confirmed that p-wave coupling was higher than s-wave, and that indeed p-wave coupling at  $60^\circ$  angle of incidence was better than that at normal incidence. This is illustrated in Figure 3 which shows (above) the cases achieved with p- and s-waves at  $60^\circ$  and (below) those achieved when the beams were brought to normal incidence. Conditions were adjusted so that the applied power density at the surface, and the interaction time, were the same for each run.

The time-dependent temperature v. depth profile (and therefore the hardening of the case) is controlled through the power density and the interaction time (inversely proportional to the scan speed) of the laser beam<sup>(7)</sup>. In particular, the temperature gradient must be such that the full case depth is austenitised whilst the surface temperature must not exceed the melting point. The typical conditions of applied power density found in this work were  $4\text{kWcm}^{-2}$  and  $2\text{kWcm}^{-2}$  for steel and iron respectively.

A total of five absorbing coatings were assessed: colloidal graphite, manganese phosphate<sup>(8)</sup>, Tufftride<sup>(9)</sup>, Wellcoat 122<sup>(10)</sup> and complex steam produced oxide (principally  $\text{Fe}_3\text{O}_4$ ). The last four have the merit of providing a uniform, cosmetically attractive, scuff-resistant coating on the component.

Spray-applied colloidal graphite was found to be the most consistently reliable coating; it is easy to apply, previous work<sup>(11)</sup> indicates that it offers ~80% absorptivity, and the laser treated surface is readily cleaned.

With manganese phosphate there was some evidence that when laser conditions were chosen to create deeper ( $\sim 0.75\text{mm}$ ) cases in steel, a fine crazing of the surface with random shallow pitting appeared. This is shown in the left hand side of Figure 4, where the cracks extend to a depth of  $\sim 60\mu\text{m}$ . The effect is believed to be associated with the



formation of iron phosphides at the grain boundaries. It was found possible to machine off the crazed layer, but this would introduce an extra manufacturing operation.

The laser absorptivity of Tufftride was assessed for two batches of cast iron (which received separate pre-coating), and for one batch of steel. The steel and one of the cast irons exhibited very poor coupling (as evidenced by shallow cases) whilst the other cast iron batch exhibited coupling almost as good as that with colloidal graphite.

Wellcoat 122 is a coating developed primarily for treatment of aluminium alloy. Its laser absorptivity was assessed for two separately-coated batches of steel and two batches of iron. Both sets of iron exhibited cases comparable to those achieved with colloidal graphite, but the results for steel were poor: the first batch exhibited only a shallow case, and the second exhibited no hardening at all.

Finally, steam oxide was investigated for steel. This black coating is produced by heating the component to  $\sim 600^{\circ}\text{C}$  and then exposing it to super-heated steam. This thermal cycle can provide useful stress-relief. However, the coupling efficiency, as judged by the case depth produced, was variable. This appeared to be associated with crazing and spallation of the coating. The right hand side of Figure 4 shows a replica of a laser treated surface where the break-up of the layer is clearly seen.

In summary, some of the best coupling, and certainly the best reproducibility, was found with colloidal graphite and it was used in most of the subsequent trials. The mixed results obtained with the other coatings have been a disincentive to their further use at this stage; nevertheless, there may be scope to more fully understand and optimise use of some of these coatings.

#### 4.2 Metallurgy

The compositions of the two materials investigated are shown in Table 1, and Figure 5 (upper) shows the microstructures. The nodular cast iron is in two conditions (a) quenched and tempered, with an acicular, tempered martensite structure of hardness  $\sim 320\text{HV}_{10}$ , and (b) normalised. The steel is of a 0.4%C direct hardening type in quenched and tempered condition, the microstructure again being of an acicular, tempered martensite form, hardness of  $\sim 260\text{HV}_{10}$ , with some non-metallic inclusions present.

Optimised hardening conditions were applied to all three colloidal graphite coated materials and Figure 5 (lower) shows microstructures near the hardened surfaces. All materials exhibit fully martensitic structures with no evidence of surface melting, cracking, dissolution of the graphite nodules or autotempering. Microhardness measurements are

shown in Figure 6 taken on samples having similar case depths. Both irons show similar response, although the normalised structure has slightly more hardness variation. The lower carbon content steel has a lower hardness but with little scatter on the results. It is proposed that in production, hardened pistons will be lightly tempered to reduce these high as-treated hardnesses, and also to help reduce any hardening stresses.

#### 4.3 Geometrical Aspects

A rectangular beam pattern was used in this work, where the intensity distribution dipped somewhat in the centre as a consequence of the simple harmonic motion of the vibrating mirror system and the use of a rectangular mask to define the usable beam. The distribution, when applied to a semi-infinite coupon, produces a substantially flat-bottomed case as shown for example in Figure 3, and an experimental investigation was undertaken to see how well it would cope with the present special case of the treatment of an edge. Figure 7 shows the results for cast iron coated with colloidal graphite. The circular test piece was mounted eccentrically on the turntable so that during rotation its sharp edge experienced radial run-out with respect to the fixed laser beam. Transverse sections taken at a number of peripheral positions on the sample are shown in Figure 7 in terms of their radial offset between outer beam flank and the edge. The sections range from that shown at the bottom of the figure, where the beam is too far inside the edge so that no hardening occurs there, to that shown at the top where excessive energy is incident on the edge and it melts. The case produced with a radial offset of + 0.5mm is regarded as ideal and the inferred tolerance on alignment of approximately  $\pm 0.5\text{mm}$  is not regarded as unduly demanding.

Similar results were obtained on steel which is indeed easier to treat because of the larger gap between austenitising temperature and melting point. In both steel and cast iron, measurements indicated that hardness was maintained right up to the edge i.e. self-quenching was sufficient, and air-jet quench or bolt-on chill blocks were unnecessary.

## 5. APPLICATION TO COMPONENTS

### 5.1 Back Tempering

Full treatment of the groove side-face in a complete piston requires that the beam must end up overlapping its starting point. In this region, back tempering will occur, and there may be the possibility of cracking. To assess this, groove side-faces were hardened with a 10mm peripheral overlap of finish and start, where the beam was switched off using the standard laser shutter having a closing time of 200ms. No cracking was seen in either steel or iron. Figure 8 shows a longitudinal section at the overlap for steel, together with a microhardness scan carried out just below the surface. It is seen that the sub-surface hardness of the prior-hardened case is locally reduced at the overlap from its usual value of approximately 800HV<sub>0.2</sub>, but that it falls below a level of 500HV<sub>0.2</sub> for a peripheral distance of only approximately 1.6mm. It was found that the extent of the tempering could be somewhat reduced by activating, at the moment of beam switch-off, a jet of compressed air which was directed at the heating point. Figure 8 shows that the peripheral distance having hardness below 500HV is now only approximately 1.3mm. It is believed that these limited regions of back-tempering will have no deleterious effect on piston performance.

Tempering was also anticipated where treatment of a groove side-face could affect an adjacent, previously-hardened face. Clearly the degree of tempering will depend on the mass of metal separating the two side-faces, and on the beam energy input. Figure 9 shows results of an experimental assessment of a 'worst-possible' situation in cast iron where the faces are separated by just 8mm, and where the treatment speed was rather slower than that normally used. Tempering-back by 100-150HV<sub>0.2</sub> has occurred but the minimum hardness is still approximately 800HV<sub>0.2</sub>.

### 5.2 Assessment of Distortion and Surface Changes

Careful assessment is being made of component distortion in view of the attractions of treating finish-machined components, and of the stringent dimensional specifications. The present indications are that dimensional changes resulting from laser treatment are minimal, provided that a high-temperature stress relief is employed at the appropriate



stage in machining, and provided that the volume of transformed material is low. Measurements indicate that a reduction of a few microns in groove width takes place, but that this is reproducible and therefore compensation can be made during machining. It may be noted that this surface expansion is consistent with that expected for martensitic transformation in a 0.5mm case.

The surface topography also remains essentially unchanged. This is shown in Figure 10 for a laser-treated steel piston, where it is seen that the characteristics of the preferred single-point turned groove finish (typically 0.5 micron Ra) are precisely retained.

### 5.3 Production Components and Field Trials

Nodular cast iron pistons of 250mm diameter and a number of steel crowns in the size range of 190-400mm diameter have been successfully treated without serious difficulty (Figure 11). After hardening, and before the components were subjected to a low-temperature stress-relief (typically 200°C), the grooves were cleaned to remove any degraded laser-absorptive coating. Although the cleaning was slightly troublesome for some of the conversion coatings described, it proved straightforward for the preferred colloidal graphite, and resulted in a bright and reflective surface. Full-scale engine trials will clearly take several years to complete. However, trials have commenced in two engines (275mm and 320mm bore) with pistons carrying steel crowns with laser hardened grooves. In each case only several hundred hours of operation has been achieved so far, but without problem.

## 6. CONCLUSIONS

This investigation and optimisation of the laser hardening of piston-groove side-faces has resulted in the creation of well-controlled transformed cases having appropriate geometry. Process efficiency has benefited from exploitation of beam polarisation and from assessment of a range of absorbing coatings. Treatment conditions have been developed for quenched and tempered steel, and for nodular cast iron in the quenched and tempered and the normalised condition. The metallurgical structures and hardness profiles are very satisfactory. Laser beam heating appears to cope well with the demanding requirement of treatment of a sharp edge, and edge melting can be avoided even in the more

difficult cast iron. Back-tempering associated with overlapping of the treatment finish and start is small, as is that associated with successive treatment of the two adjacent side-faces. Component distortion and surface topography changes arising from the laser treatment are minimal, indicating that treatment of final machined components is entirely feasible. A number of production piston components have received full laser treatment, and engine trials have commenced; although at an early stage, these have not identified any problems associated with the process.

The preliminary indications are that the process should be commercially, as well as technically, viable. The relatively high cost of the laser treatment (associated with equipment capital cost) may be largely offset by the demonstrated ability to treat components in the finish-machined condition without need for expensive regrinding operations. Furthermore, high utilisation of the laser is possible through rapid switching of the beam between alternate workstations. Additionally, laser hardening copes well with the treatment of a wide range of component sizes and will, possibly, permit the retreatment of service-worn components due to the low internal stress generated.

## 7. ACKNOWLEDGEMENTS

This work was supported by the UK Department of Trade and Industry, and acknowledgement is made of the assistance of R.A. Day and colleagues at Wellworthy Ltd, and of colleagues within the Culham Laser Applications Group.

## 8. REFERENCES

- (1) AV La Rocca. Laser Applications in Manufacturing. Scientific American, March 1982, 80-87.
- (2) Laser Report, Penn Well Publ., April 30th 1984.
- (3) RM Macintyre. Proc. Conf. Lasers in Materials Processing, Los Angeles, Jan 1983. Ed. E.A. Metzbower, ASM, pp230-239.
- (4) JE Miller, JA Wineman. Laser hardening at Saginaw Steering Gear. Metal Progress, May 1977, 111, 38.
- (5) EJ Strong. Laser Focus/Electro Optics, Nov 1983, 172-180.
- (6) MI Arzuov et al. Some features of laser heating of oxidizable metals in air by oblique incident radiation. Sov. J. Quantum Electron. 9(10), Oct 1979, 1308-1310.

- (7) DNH Trafford, T Bell, JHPC Megaw, AS Bransden. Laser treatment of grey iron. Proc. Conf. Heat Treatment '81, Birmingham, Sept 1981. The Metals Society, 198-206.
- (8) Trade literature Pyrene Ltd, Bucks, UK.
- (9) Trade literature Degussa Ltd, Cheshire, UK.
- (10) Trade literature Wellworthy Ltd, Hampshire, UK.
- (11) DNH Trafford, T Bell, JHPC Megaw, AS Bransden. Heat treatment using a high power laser. Proc. Conf. Heat Treatment '79, Birmingham, May 1979. The Metals Society, 32-38.



	C	Si	Mn	Cu	Cr	Mo	Mg	S	P
Steel	0.4	0.2	0.6	0.6	1.2	0.3	-	0.08	0.03
Cast Iron	3.4	2.2	0.3	0.6	0.5	0.05	0.05	0.01	0.03

Table 1. Composition (typical analysis) of piston steel and cast iron.

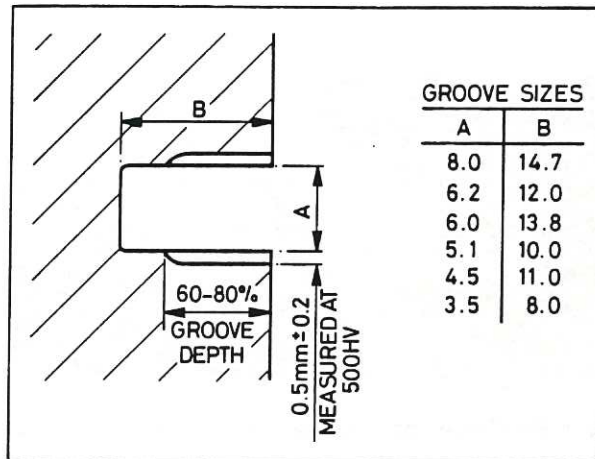


Figure 1. Groove hardening target specification and typical groove sizes.

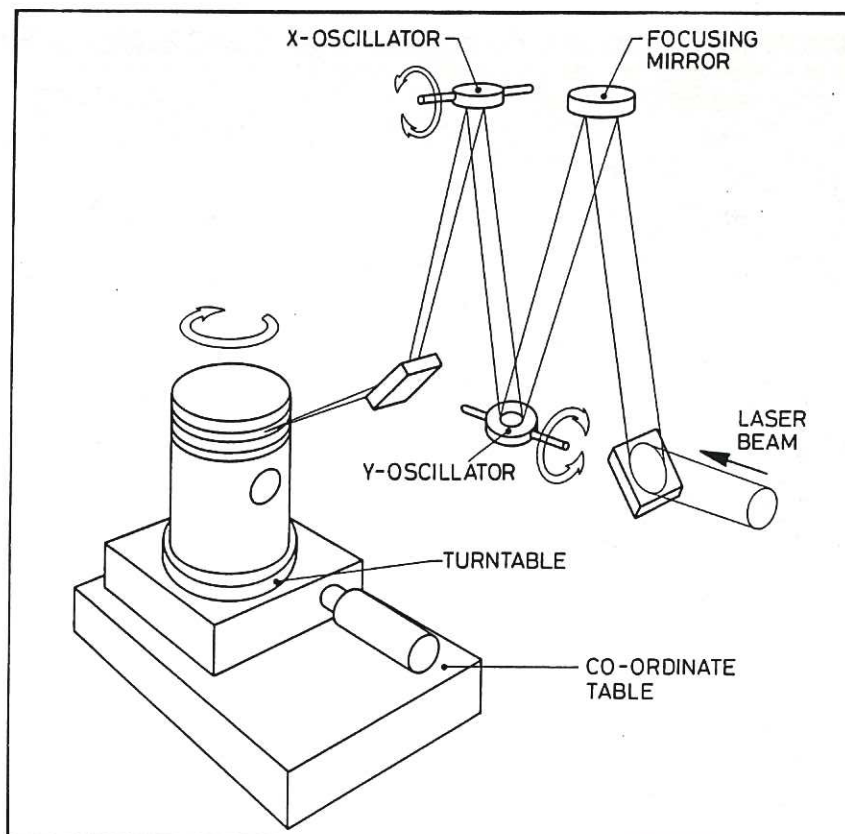


Figure 2. Schematic of beam and workpiece manipulation.

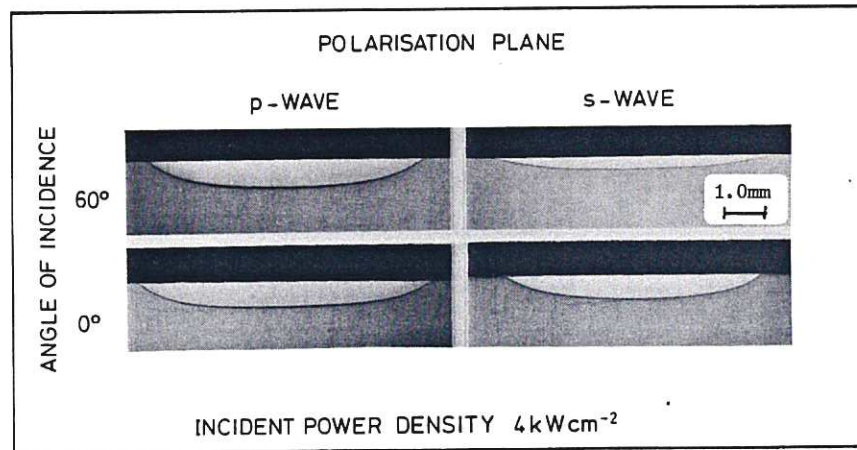


Figure 3. Effect on absorptivity of polarisation plane and angle of incidence.

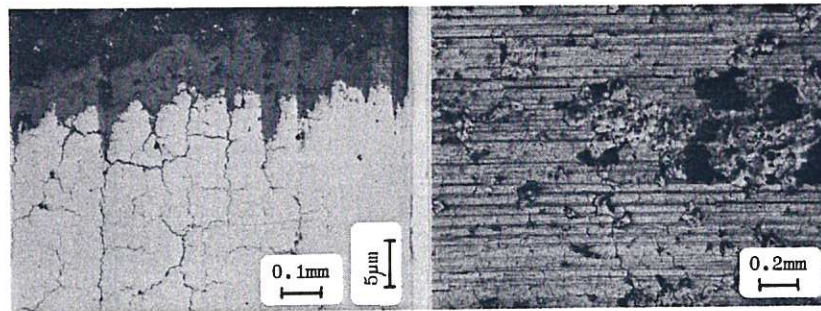


Figure 4. Left: Surface cracking seen on laser-treated manganese phosphate coated steel (taper section). Right: Crazing and spalling of steam oxide coating after treatment (shown by replica technique where black areas are detached coating adhering to replica).

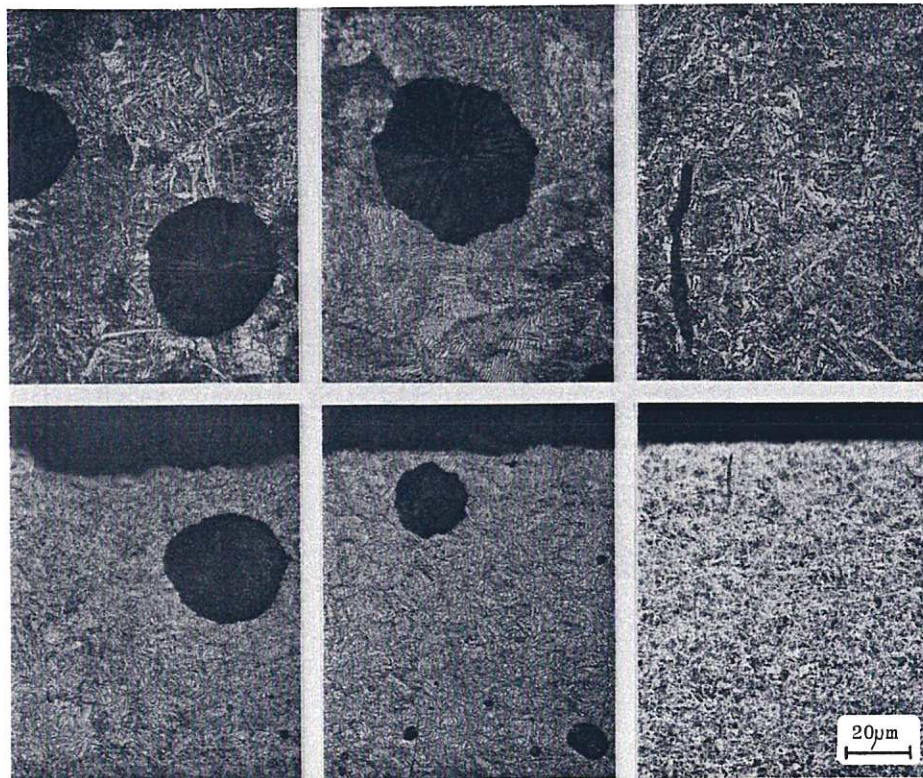


Figure 5. Microstructures of parent material (above) and laser hardened (below) showing from left to right, quench/tempered cast iron, normalized cast iron and quench/tempered steel.



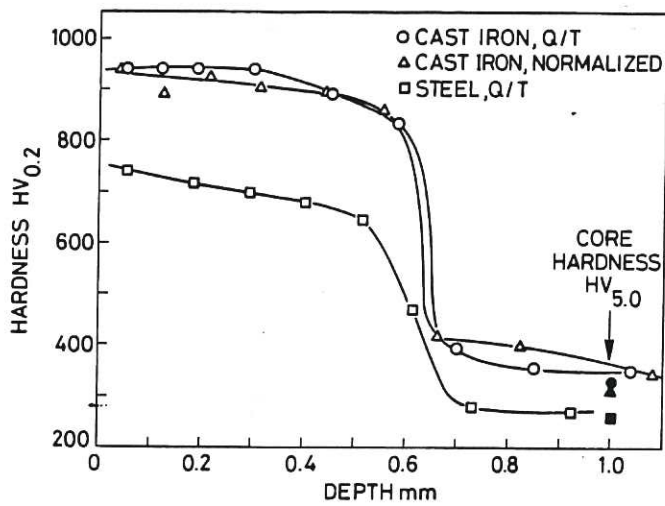


Figure 6. Typical microhardness profiles of the three materials, as hardened.

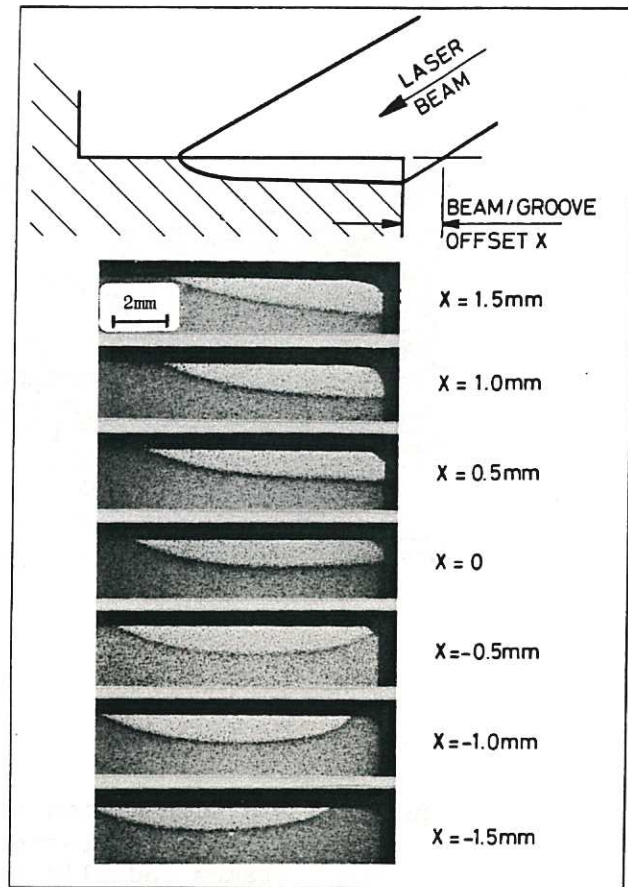


Figure 7. Effect of beam positioning on case geometry.

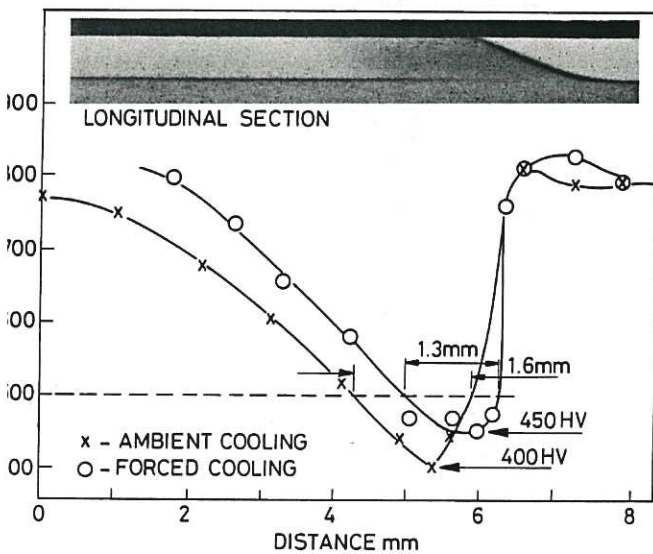


Figure 8. Tempering of previously hardened layer at overlap region in steel showing beneficial effect of forced air cooling. Hardness measurements taken 0.1mm below surface.

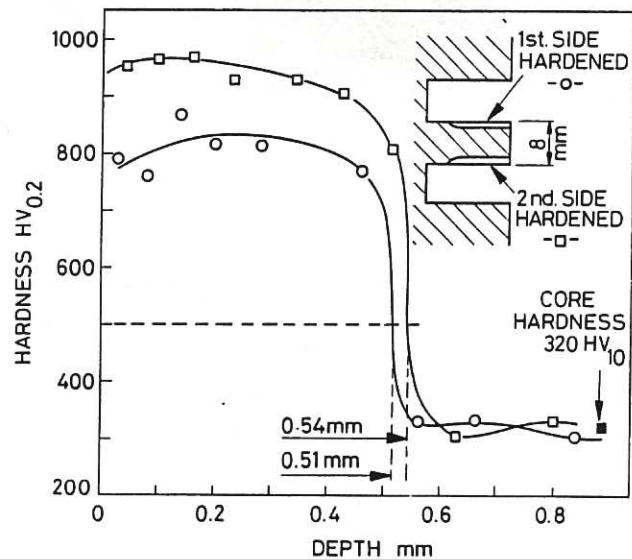


Figure 9. Tempering effect on hardened face in cast iron caused by treatment of adjacent second face. (Note that these hardnesses will be reduced in subsequent stress relief cycle).



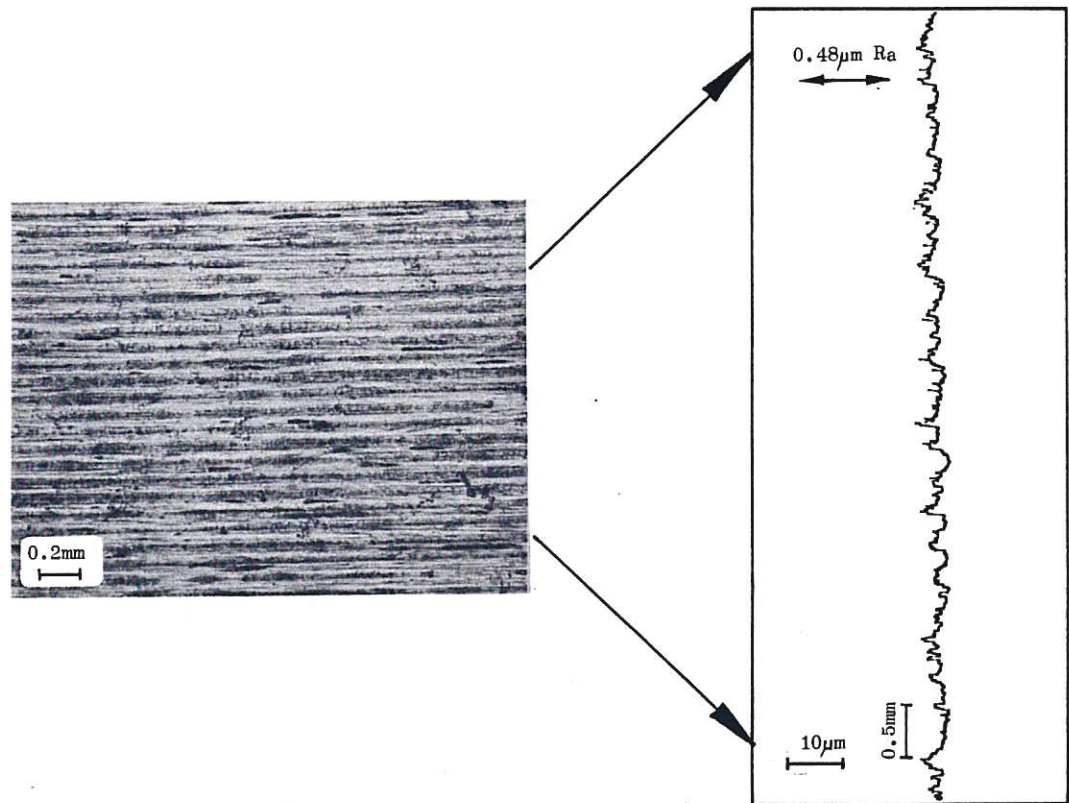


Figure 10. Surface finish of treated groove showing (left), surface appearance and (right), Talysurf measurement taken radially across hardened groove.



Figure 11. Typical pistons hardened - foreground, 190mm  $\phi$  steel crown and background, 325mm  $\phi$  steel crown (left) and 250mm  $\phi$  cast iron monolithic. Inset shows a hardened cast-iron groove in section.





